The 1st International Symposium on Multi-Robot and Multi-Agent Systems (MRS 2017)
December 4-5, 2017, Los Angeles, CA, USA

Distributed Multi-Robot Localization from Acoustic Pulses Using Euclidean Distance Geometry

Trevor Halsted[1] and Mac Schwager[2]

***Abstract*— This paper presents a method for reconstructing relative positions of a group of robots from only acoustic pulses sent and received by the robots. The approach is fully distributed—each robot calculates relative positions from its measurements alone—and does not require any additional communication between the robots outside of the acoustic pulses. The method applies concepts from Euclidean distance geometry to label each robot's measurements, constructing first a set of relative distances and then a set of relative positions. We also implement two practical methods for aligning a robot's estimated set of relative positions in a global frame of reference. Due to the minimal sensing and communication requirements, this approach to multi-robot localization is appropriate for underwater applications and other environments in which traditional communication channels are limited, untrustworthy, or unavailable.**

I. Introduction

Many tasks that involve the collaboration of multiple robots require a reliable method of determining the robots' positions relative to each other. Examples of multi-robot tasks that require relative positions include mapping [1], target tracking [2], and manipulation [3]. Typically, implementing these cooperative applications requires sensing the positions of the robots (such as from vision sensors, global positioning, range sensors, etc.) and sharing the information, either through a distributed protocol involving a communication network among the agents, or with a centralized controller.

Although these approaches have found use in a variety of settings, scenarios exist for which communication and sensing constraints are incompatible with these standard methods. For instance, in underwater multi-robot applications [4], localization is typically hindered by the opacity of water to most frequencies of electromagnetic wave (required for GPS localization and long-range radio communication), necessitating lower-bandwidth acoustic-based communication [5]. Therefore, it is of interest to consider the development of a localization method that is not only fully distributed, but also well-suited for environments with constrained sensing and communication.

This paper addresses the problem of reconstructing the relative positions of a group of robots using only times-of-arrival of acoustic pulses that are propagated among the robots. The localization method is fully distributed, meaning that each robot independently reconstructs the system's formation from its own measurements. Furthermore, our approach does not require robot-to-robot communication beyond the sending and receiving of acoustic pulses at several frequencies and in most cases a synchronized clock.

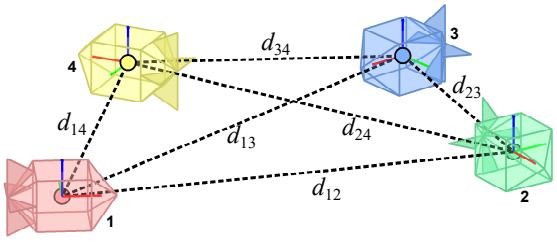

Fig. 1: In order for each robot to independently localize the whole system from only acoustic information (i.e., determine positions $\boldsymbol{x} = [\boldsymbol{x}_1 \quad \boldsymbol{x}_2 \quad \boldsymbol{x}_3 \quad \boldsymbol{x}_4]$), it must reconstruct all pairwise relative distances $\{d_{12}, d_{13}, d_{14}, d_{23}, d_{24}, d_{34}\}$ and orient the rigid structure in a known coordinate frame.

A. Related Work

Beginning with the introduction of distributed localization as a way to improve pose estimations among a group of robots [6], a variety of methods for localization of single- and multi-robot systems have emerged. In one of the earlier works in localization and mapping with only distance measurements, Newman and Leonard demonstrate the navigation of a single autonomous underwater vehicle (AUV) using acoustic time of flight with stationary beacons [7]. In [8], the authors propose expanding the range-only map by using odometry to increase the likelihood of obtaining a rigid graph. In contrast to these methods' assumption of only one moving member of the robot-beacon system, our approach places no constraints on the relative motion of the robots.

Work in [9] states necessary conditions for uniquely determining relative robot positions based on relative distance measurements at different times (as well as odometry measurements that are shared between the robots). Additional fundamental geometric concepts are introduced in [10], namely the "robust quadrilateral"—a graph for which edge lengths uniquely produce a set of relative positions.

In [11], the authors present a localization and navigation problem involving multiple moving AUVs and a single accompanying surface craft. Acoustic signals between the AUVs allow them to use each other as mobile beacons for localization. More recently, [12] extends range-based localiza-

[1]Trevor Halsted is with the Department of Mechanical Engineering, Stanford University, Stanford, CA 94305, USA halsted@stanford.edu

[2]Mac Schwager is with the Department of Aeronautics & Astronautics, Stanford University, Stanford, CA 94305, USA

This work was supported in part by a Stanford Graduate Fellowship, an NDSEG Fellowship, NSF grant CMMI-1562335, and ONR grant N00014-16-1-2787.

tion to robot swarms operating with minimal communication and [2] applies relative localization techniques to a target-tracking application. Even compared to the low-bandwidth communication in these methods (e.g., a 32byte/10s acoustic modem in [11]), our approach requires only a small set of acoustic pulses to be sent and received among robots. We propose an Acoustic Echoing Protocol (AEP), by which a combination of acoustic pulses is sufficient for each robot to reconstruct the relative positions of all robots.

A subset of range-based localization techniques exploit the properties of Euclidean distance matrices (EDMs), which are matrices containing squared pairwise relative distances among a set of points, to reconstruct formation estimates from noisy measurements. For example, [13] addresses the completion problem (reconstructing all pairwise relative distances from incomplete measurements) for the purpose of localizing a receiver in a wireless network. Similar completion problems typically involve a setup in which only some of the sensors have known positions ("anchors"), and the entire network is localized globally based on relative distances to these anchors [14][15]. Additionally, several works provide the general foundational tools for exploiting the properties of EDMs in localization problems [16][17]. This class of problems generally involves recovering correct distance matrices from measurements that are noisy, missing, or unlabeled. Our approach extends this work to address the problem of robots in a network performing EDM completion from their own measurements.

Our approach also uses similar techniques to recent research in acoustic room reconstruction. In particular, Dokmanić et al. address "hearing" the shape of a room (deducing the locations of its walls from the times of arrival of echoes) with a variety of microphone and speaker configurations [18][19][20][21]. In [22], an array of microphones tracks a moving acoustic source without direct line-of-sight. Similar work addresses echo-based simultaneous localization and mapping in [23], [24], and [25]. In practice, room reconstruction can be framed as a problem of localizing a set of "virtual nodes" (as introduced in [26]). Our approach extends several techniques from room reconstruction to the task of localizing a set of mobile robots from a signal that contains acoustic echoes sent by the robots.

B. Contributions

This paper addresses several challenges in extracting relative position information from an acoustic signal. First, because our method uses no direct sharing of information, each robot must obtain all pairwise relative distances from the acoustic signal only (i.e., each robot shown in Figure 1 must deduce times of arrival for paths that include all six of the robot-to-robot distances), which distinguishes this approach from typical range-only localization methods. The Acoustic Echoing Protocol that we introduce is simple: each robot sends a single pulse at its own frequency, and the first time it hears each other robot's frequency, it repeats ("echoes") a pulse at that same frequency.

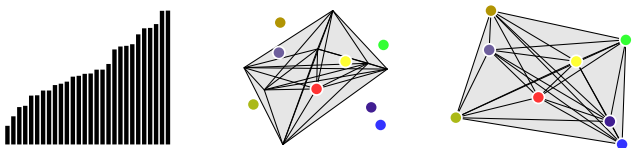

(a) (b) (c)

Fig. 2: Visualization of localization steps: (a) collecting distances, (b) finding correspondence of edges to nodes to form a rigid structure, and (c) aligning the rigid structure to a reference frame.

Second, given the acoustic signal that each robot records, the next step is to determine the correspondence between each pulse's time of arrival and the path by which the pulse travels. Equivalently, the approach extracts a set of distances and embeds them in a rigid formation (e.g., taking the lengths in Figure 2a to construct the structure in Figure 2b). We introduce two algorithms to solve an "echo sorting" problem similar to those in the acoustic room reconstruction literature [17][19].

The final challenge in the localization problem is visualized in the transformation on the structure in Figure 2b to produce that in Figure 2c. Each robot must determine the orientation of the formation that it recovers in the previous step. We present two practical approaches to this "anchoring" problem. While the simulations in this paper assume a multi-robot system operating in two-dimensions,the algorithms and theory we present apply in Euclidean spaces of arbitrary dimension.

II. Acoustic Echoing Protocol

Consider n robots with positions $\boldsymbol{x}_i \in \mathbb{R}^m$, $i = 1, \ldots, n$. The distance between robots i and j is denoted as $d_{ij} = \|\boldsymbol{x}_j - \boldsymbol{x}_i\|$. We represent the collection of n position vectors as a matrix $\boldsymbol{X} = [\boldsymbol{x}_1 \ \cdots \ \boldsymbol{x}_n]$, $\boldsymbol{X} \in \mathbb{R}^{m \times n}$. Each robot can send and receive acoustic pulses at n different frequencies f_i, and each frequency f_i is identified with an associated robot i[1]. Let the set of times that robot i receives a pulse at frequency f_j during a single round of sending and receiving be denoted as $\boldsymbol{t}_j^i = \left[t^i_{j(1)}, t^i_{j(2)}, \ldots\right]$. The time of each robot's initial transmission is denoted as τ_i. Also, define $\Delta_t \geq 0$ as a constant delay time.

We propose an Acoustic Echoing Protocol (AEP, Algorithm 1), in which each robot sends a pulse at its own frequency, then echoes every other robot's frequency once, as illustrated in Figure 3 for 4 robots. We let the AEP proceed in rounds, with each round lasting long enough for all robots to receive all echoed pulses. Each robot i sends a pulse of frequency f_i at time τ_i (Figure 3a). In the synchronous implementation of the AEP, the robots possess synchronized clocks, and τ_i is a scheduled time of transmittance. When a pulse of frequency f_j arrives at robot i, robot i records

[1]Note that we assume that the robots' speeds are slow enough and the signaling frequencies are sufficiently separated so that the Doppler effect is insignificant. For instance, even robots moving as fast as 10m/s underwater would only experience a maximum frequency distortion of 1.4%

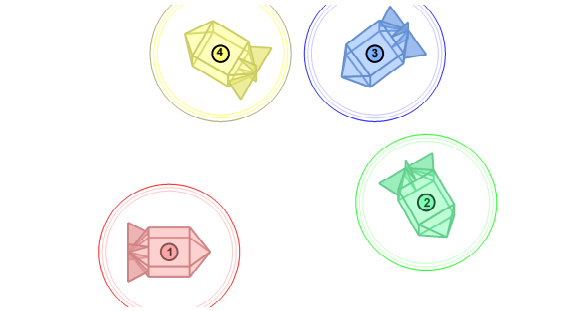

(a) $t = 0.004$s

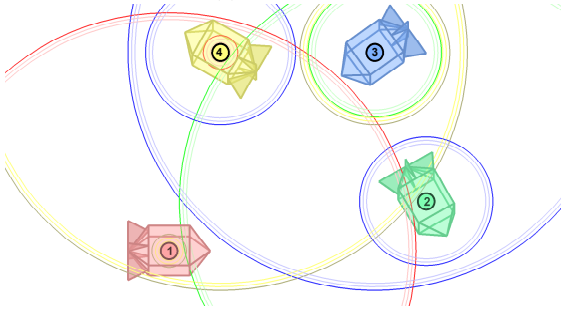

(b) $t = 0.014$s

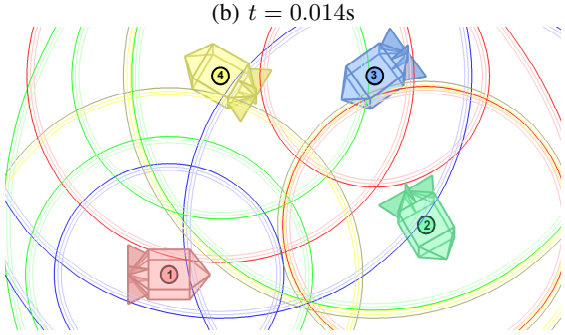

(c) $t = 0.024$s

Fig. 3: Propagation of echoes for a four-robot system with synchronous timing ($\tau_i = \tau_j, \{i, j\} \in \{1, \ldots, n\}$), with each robot performing Algorithm 1 in a 5m $\times$ 5m space.

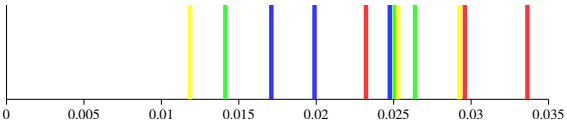

Fig. 4: Times of arrival of acoustic pulses, heard by robot 1 (red) during the Acoustic Echoing Protocol simulation shown in Figure 3

the time of arrival in $\boldsymbol{t}_j^i$. Upon receiving the first-arriving pulse at f_j in the current round and waiting a delay Δ_t, robot i sends an "echo" pulse at f_j (e.g., in Figure 3b). For a system of n robots, there are n initial pulses and $n(n-1)$ echoed pulses (Figure 3c). Each robot records $(n-1)$ signals at each of the n frequencies in one round of the AEP, as in Figure 4. The arrival times contain sums of combinations of robot-to-robot distances, of which there are $n(n-1)/2$ in total. However, the correspondence between the arrival times of these pulses and their associated paths is ambiguous. Therefore, the AEP provides each robot with sufficient (though unlabeled) information to calculate all relative distances among the robots.

Algorithm 1 Acoustic Echoing Protocol for Robot i

function AEP($i, n, \tau_i^i, \Delta_t, t_{\text{end}}$)
  Send f_i at time τ_i^i ▷ Initial pulse
  while $t < t_{\text{end}}$ **do**
    for $j = \{1, \ldots, n\}$ **do**
      if Robot receives first pulse at f_j **then**
        $t^i_{j(1)} \leftarrow t$
        Send f_j at $t = t^i_{j(1)} + \Delta_t$ ▷ Echo pulse
      end if
      if Robot receives subsequent pulse at f_j **then**
        $t^i_{j(q+1)} \leftarrow t$ ▷ $q+1$ is next element of $\boldsymbol{t}^i_j$
      end if
    end for
  end while
  return $\boldsymbol{t}^i_1, \ldots, \boldsymbol{t}^i_n$ ▷ All times of arrival
end function

III. Recovering Relative Distances

After each robot i operates Algorithm 1 to acquire the set of all times of arrival for each frequency $\{\boldsymbol{t}^i_1, \ldots, \boldsymbol{t}^i_n\}$, it reconstructs relative distances from this noisy acoustic signal.

For the set of n points in $\mathbb{R}^m$, define $\boldsymbol{D} \in \mathbb{R}^{n \times n}$ such that the (i, j) element is the squared distance between point i and point j: $d_{ij}^2 = \|\boldsymbol{x}_i - \boldsymbol{x}_j\|^2$. $\boldsymbol{D}$ is a symmetric matrix with all elements greater or equal to zero and with zeros on its diagonal ($d_{ij} = d_{ji}$, $d_{ii} = 0$). Importantly, if we construct $\boldsymbol{D}$ from a set of points in dimension m ($\boldsymbol{x}_i \in \mathbb{R}^m$, $i = 1, \ldots, n$), then the following is true [17]:

$$\text{rank}(\boldsymbol{D}) \leq m + 2. \tag{1}$$

If the number of points n (corresponding to the size of $\boldsymbol{D}$) exceeds the dimension of the space by $n > m + 2$, then computing $\boldsymbol{D}$ will produce a matrix that is not of full rank. Consequently, we can use (1) to determine whether a zero-diagonal symmetric matrix is in fact an EDM[2] (that is, if it corresponds to squared relative pairwise distances for a set of n points in $\mathbb{R}^m$). However, for $\tilde{\boldsymbol{D}}$ constructed of noisy distance measurements between n points in $\mathbb{R}^m$, (1) no longer holds. In general, we model the measurement uncertainty as additive Gaussian noise on the distances: the (i, j) element of $\tilde{D}$ is $\tilde{d}_{ij}^2 = (d_{ij} + \delta)^2$, $\tilde{d}_{ij}^2 = \tilde{d}_{ji}^2$. Instead of the rank condition (1), we use a condition number test of $\tilde{\boldsymbol{D}}$ to determine if it approximates a matrix that satisfies (1).

Given the speed of sound c of the medium in which the robots operate (e.g., $c = 1481$m/s in water at 20°C), we define the measured length of the path that a pulse travels to be proportional to its time of arrival as $l^i_j = ct^i_j$. Let $\boldsymbol{L}^i \in \mathbb{R}^{(n-1)\times n}$ tabulate the path lengths that node i measures, with column $\boldsymbol{l}^i_j$ containing $l^i_{j(1)}, \ldots, l^i_{j(n-1)}$. Determining the assignment of the paths means for each $\boldsymbol{l}^i_j$ finding the map between the sets $\{l^i_{j(1)}, \ldots, l^i_{j(n-1)}\}$ and $\{d_{j1} + d_{1i}, \ldots, d_{jn} + d_{ni}\}$. We can show that determining

[2]Note that (1) is a necessary but not sufficient condition for a matrix to be an EDM; as a trivial example consider $-\boldsymbol{D}$, which has the same rank as $\boldsymbol{D}$ but cannot be an EDM because its elements are not positive.

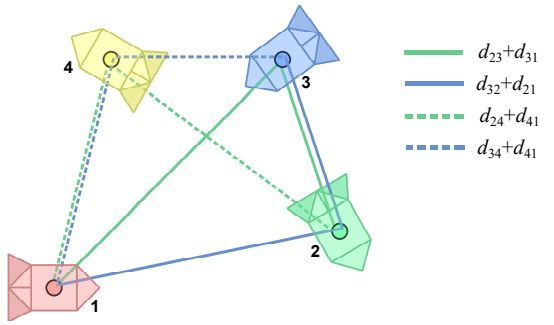

Fig. 5: The measurements from which robot 1 (red) determines the distance between robots 2 and 3 (green and blue). Echo sorting is required to determine which two measurements correspond to paths that include d_{23}.

the correspondence between the measured path lengths and the nodes through which each path passes is equivalent to reconstructing a noisy distance matrix $\tilde{\boldsymbol{D}}$. Consider $\boldsymbol{E}^i \in \mathbb{R}^{n\times n}$, which tabulates a redundant set of one- and two-edge paths to robot i, as illustrated for node 1 in (2).

$$\boldsymbol{E}^1 = \begin{bmatrix} 0 & d_{12}+d_{21} & d_{13}+d_{31} & \cdots & d_{1n}+d_{n1} \\ d_{21} & d_{21} & d_{23}+d_{31} & \cdots & d_{2n}+d_{n1} \\ d_{31} & d_{32}+d_{21} & d_{31} & \cdots & d_{3n}+d_{n1} \\ \vdots & \vdots & \vdots & \ddots & \vdots \\ d_{n1} & d_{n2}+d_{21} & d_{n3}+d_{31} & \cdots & d_{n1} \end{bmatrix} \tag{2}$$

Lemma 1: If robot i can correctly sort the measured path lengths $\{l^i_{j(1)}, \ldots, l^i_{j(n-1)}\}$ for all $j \in \{1, \ldots, n\}$ to construct $\boldsymbol{E}^i$, then it can also determine $\tilde{\boldsymbol{D}}$ containing noisy squared distances.

Proof: Consider the operator $\boldsymbol{C}_i = \boldsymbol{I} + \mathbf{1}\boldsymbol{i}_i^T$ ($\boldsymbol{i}_i$ is the ith column of $\boldsymbol{I}$). $\boldsymbol{C}_i^{-1} = \boldsymbol{I} - (1/2)\mathbf{1}\boldsymbol{i}_i^T$. $\boldsymbol{C}_i$ maps between $\boldsymbol{E}^i$ and $\sqrt{\boldsymbol{D}}$, the element-wise square root of $\boldsymbol{D}$: $\boldsymbol{C}_i\sqrt{\boldsymbol{D}} = \boldsymbol{E}^i$ and $\sqrt{\boldsymbol{D}} = \boldsymbol{C}_i^{-1}\boldsymbol{E}^i$. ■

Therefore, the AEP produces an acoustic signal that contains enough information to reconstruct $\tilde{\boldsymbol{D}}$.

A. Echo Sorting Algorithm

Assuming that timing among the robots is synchronous (that is, $\tau_i = \tau_j$ for all $i, j \in \{1, \ldots, n\}$), each robot i can populate $\boldsymbol{E}^i$ and $\tilde{\boldsymbol{D}}$ with the first-arriving pulses at each frequency as the direct-path distances. However, the correspondence of the remaining pulses to the paths is not immediately apparent. Algorithm 2 exploits the redundancies in $\boldsymbol{E}^i$ to sort these echoes. For instance, consider robot i finding d_{jk}. There are two measurements of paths that contain this distance (with noise): the quantity $d_{jk} + d_{ki}$ in $\boldsymbol{l}^i_j$ and $d_{kj} + d_{ji}$ in $\boldsymbol{l}^i_k$. Figure 5 illustrates this redundancy for robot 1 determining d_{23}. Algorithm 2 chooses as d_{jk} the closest match between the vectors $\left(\boldsymbol{l}^i_j - \mathbf{1}d_{ki}\right)$ and $\left(\boldsymbol{l}^i_k - \mathbf{1}d_{ji}\right)$ by comparing $(n-2)^2$ candidate combinations for each of the $n(n-1)/2$ unknown distances.

B. Asynchronous Timing

We observe that in a system containing three robots, each robot evaluates only one candidate for the estimated distance between the other two robots. Consequently, we can solve the distance matrix deterministically, even when $\tau_1 \neq \tau_2 \neq \tau_3$ (i.e., each of the three robots initializes its pulse at an unknown time). Algorithm 3 returns not only $\tilde{\boldsymbol{D}}$ but also the relative timing offsets. The algorithm takes advantage of the fact that the two paths that contain a particular distance d_{jk} ($d_{jk} + d_{ki}$ and $d_{kj} + d_{ji}$) include $c\tau_j$ and $c\tau_k$, respectively. As a result, comparing the two estimates of d_{jk} eliminates the uncertainty from the timing offsets. Algorithm 3 enables the three-robot system to localize from acoustic pulses that are initialized asynchronously, or alternatively to synchronize clocks without additional communication.

While the approach in Algorithm 3 is unique to the case of $n = 3$, we can also approach asynchronous echo sorting for a larger group of robots ($\tau_j \neq \tau_k$ for $j, k \in \{1, \ldots, n\}$). However, for $n > 3$, we must first resolve the unknown timing offsets and then apply Algorithm 2 to assign distances. Robot i can determine the unlabeled set of direct-path distances (d_{ij} for $j \in \{1, \ldots, n\}$) from measurements taken at frequency f_i and the labeled set of direct-path distances with unknown offsets from first-arriving pulses at all other frequencies. Determining τ_j for $j \in \{1, \ldots, n\}$ requires finding the correspondence between these two sets

Algorithm 2 Echo Sorting

function SORTECHOES($i, \boldsymbol{L}^i$)
  $\boldsymbol{m} \leftarrow [1, \ldots, i-1, i+1, \ldots, n]$
  $\hat{\boldsymbol{D}}_{[i,\boldsymbol{m}]} \leftarrow \boldsymbol{L}^i[1, \boldsymbol{m}]$
  $\hat{\boldsymbol{D}}_{[\boldsymbol{m},i]} \leftarrow (\boldsymbol{L}^i_{[1,\boldsymbol{m}]})^T$
  for $\{j, k\} \in \{1 \ldots n\}$, $j < k$, $j \neq i$, $k \neq i$ **do**
    $\tilde{\boldsymbol{d}}_j \leftarrow (\boldsymbol{L}^i_{[2\cdots(n-1),j]} - L^k_{[1,k]})$
    $\tilde{\boldsymbol{d}}_k \leftarrow (\boldsymbol{L}^i_{[2\cdots(n-1),k]} - L^k_{[1,j]})$
    Select $d_{jk} \in \tilde{\boldsymbol{d}}_j$, $d_{kj} \in \tilde{\boldsymbol{d}}_k$ to minimize $|d_{jk} - d_{kj}|$
    $\hat{D}_{[j,k]}, \hat{D}_{[k,j]} \leftarrow (d_{jk} + d_{kj})/2$
  end for
  return $\tilde{\boldsymbol{D}}$ ▷ element-wise square of $\hat{\boldsymbol{D}}$, $\tilde{\boldsymbol{D}} \approx \boldsymbol{D}$
end function

Algorithm 3 Asynchronous Echo Sorting for $n = 3$

function SORTECHOES3($i, \boldsymbol{L}^i, \tau_i$)
  Choose $\{j, k\} \neq i$ ▷ Consider two other nodes
  $\tilde{d}_{jk} \leftarrow L^i_{[2,j]} - L^i_{[1,k]}$ ▷ $\tilde{d}_{jk} = d_{jk} + c(\tau_j - \tau_k)$
  $\tilde{d}_{kj} \leftarrow L^i_{[2,k]} - L^i_{[1,j]}$ ▷ $\tilde{d}_{kj} = d_{kj} + c(\tau_k - \tau_j)$
  $d_{jk} \leftarrow (\tilde{d}_{jk} + \tilde{d}_{kj})/2$ ▷ Cancel offsets by τ_j, τ_k
  $\hat{\boldsymbol{L}} \leftarrow [\boldsymbol{l}^i_j \; \boldsymbol{l}^i_k] - [0 \; d_{jk}]^T \mathbf{1}^T$ ▷ $\boldsymbol{L}^i = [\boldsymbol{l}^i_1 \; \boldsymbol{l}^i_2 \; \boldsymbol{l}^i_3]$
  if $\hat{L}_{[1,1]} + \hat{L}_{[2,2]} < \hat{L}_{[1,2]} + \hat{L}_{[2,2]}$ **then** ▷ $d_{ji} < d_{ki}$
    $d_{ji} \leftarrow (L^i_{[1,i]} - c\tau_i)/2$ ▷ Shorter direct path
    $d_{ki} \leftarrow (L^k_{[2,i]} - c\tau_i)/2$ ▷ Longer direct path
  else ▷ $d_{ji} \geq d_{ki}$
    $d_{ji} \leftarrow (L^i_{[2,i]} - c\tau_i)/2$
    $d_{ki} \leftarrow (L^i_{[1,i]} - c\tau_i)/2$
  end if
  Populate $\tilde{\boldsymbol{D}}$ with $d^2_{ij}, d^2_{ik}, d^2_{jk}$
  return $\tilde{\boldsymbol{D}}$, τ_j, τ_k ▷ $\tilde{\boldsymbol{D}} \approx \boldsymbol{D}$
end function

Algorithm 4 Reconstructing Positions in $\mathbb{R}^m$ from Distances

function DISTTOPOS($\boldsymbol{D}$)
  $\boldsymbol{J} \leftarrow \boldsymbol{I} - \mathbf{1}\boldsymbol{i}_1^T$ ▷ Centering Matrix ($\boldsymbol{I} = [\boldsymbol{i}_1 \cdots \boldsymbol{i}_n]$)
  $\boldsymbol{G} \leftarrow -\frac{1}{2}\boldsymbol{J}\boldsymbol{D}\boldsymbol{J}^T$ ▷ Gram matrix
  $\boldsymbol{U}, \boldsymbol{\Lambda}, \boldsymbol{V} \leftarrow SVD(\boldsymbol{G})$ ▷ $\boldsymbol{\Lambda} = \text{diag}([\lambda_{\max} \cdots \lambda_{\min}])$
  $\hat{\boldsymbol{V}} \leftarrow [\boldsymbol{v}_1 \cdots \boldsymbol{v}_m]$ ▷ Trim eigenvectors
  $\tilde{\boldsymbol{X}} \leftarrow \sqrt{\text{diag}(\lambda_1, \ldots, \lambda_m)}\hat{\boldsymbol{V}}^T$
  return $\tilde{\boldsymbol{X}}$
end function

of measurements. Noting that the terms in $\boldsymbol{l}_j^i$ (column j of $\boldsymbol{L}^i$) all share the same offset (a distance $c\tau_j$), then if ${\boldsymbol{l}_j^i}^T\mathbf{1} > {\boldsymbol{l}_k^i}^T\mathbf{1}$, it is likely that $\tau_j > \tau_k$. Thus, we compare the columns of $\boldsymbol{L}^i$ as an initial map between the robots and their respective timing offsets. We also use the condition number test of $\tilde{\boldsymbol{D}}$ to evaluate and iterate Algorithm 2 with alternate maps if there is high uncertainty. The accuracy of this approach improves with larger relative timing offsets.

IV. Recovering Relative Positions

Once each robot recovers $\tilde{\boldsymbol{D}}$ (an estimate of $\boldsymbol{D}$), it reconstructs the relative positions in two steps. First, the robot recovers some $\tilde{\boldsymbol{X}}$ in an arbitrary frame; second, the robot applies an orthogonal transformation to find the corresponding $\boldsymbol{X}$ in the desired coordinate frame.

Transforming between distances and positions involves the Gram matrix $\boldsymbol{G} = \boldsymbol{X}^T\boldsymbol{X}$. Noting that the (i,j)th element of $\boldsymbol{D}$ is $(\boldsymbol{x}_i - \boldsymbol{x}_j)^T(\boldsymbol{x}_i - \boldsymbol{x}_j)$, then $\boldsymbol{D}$ can be expanded as

$$\boldsymbol{D} = \mathbf{1}\text{diag}(\boldsymbol{G})^T - 2\boldsymbol{G} + \text{diag}(\boldsymbol{G})\mathbf{1}^T, \tag{3}$$

where $\mathbf{1}$ is a vector of ones [17]. The inverse function is

$$\boldsymbol{G} = -\frac{1}{2}\boldsymbol{J}\boldsymbol{D}\boldsymbol{J}^T, \tag{4}$$

for which $\boldsymbol{J}$ is a "centering matrix"[17] such that $\boldsymbol{J}\mathbf{1} = \mathbf{0}$. For instance, selecting $\boldsymbol{J}_{\text{cent}} = \boldsymbol{I} - \frac{1}{n}\mathbf{1}\mathbf{1}^T$ centers the point set with its centroid at the origin of the frame. Alternatively, the choice of $\boldsymbol{J}_i = \boldsymbol{I} - \mathbf{1}\boldsymbol{i}_i^T$ (where $\boldsymbol{i}_i$ is ith column of $\boldsymbol{I}$) translates the point set so that $\boldsymbol{x}_k$ lies at the origin.

From the Gram matrix, the position matrix $\boldsymbol{X}$ is found by singular value decomposition. The eigenvalues of $\boldsymbol{G}$, denoted $\lambda_1 \geq \lambda_2 \geq \cdots \geq \lambda_n$, are such that only the first m eigenvalues are nonzero, where m is the dimension. Then, given $\boldsymbol{G} = \boldsymbol{U}\boldsymbol{\Lambda}\boldsymbol{V}^T$ we find $\tilde{\boldsymbol{X}}$, centered according to the earlier choice of $\boldsymbol{J}$, as

$$\tilde{\boldsymbol{X}} = \boldsymbol{\Lambda}^{1/2}\boldsymbol{V}^T \quad \text{for a noiseless EDM } \boldsymbol{D}. \tag{5}$$

The resulting $\tilde{\boldsymbol{X}}$ reconstructs the point set $\boldsymbol{X}$ to some orthogonal transformation. In our case, after using Algorithms 2 or 3, we do not recover a noiseless EDM, but we can apply these same steps (Algorithm 4). For noisy $\tilde{\boldsymbol{D}}$ we enforce the dimension of $\boldsymbol{X}$ by trimming $\boldsymbol{\Lambda}$ and $\boldsymbol{V}$ such that

$$\tilde{\boldsymbol{X}} = \text{diag}\left(\sqrt{\lambda_1} \cdots \sqrt{\lambda_m}\right)[\boldsymbol{v}_1 \cdots \boldsymbol{v}_m]^T \quad \text{for noisy } \tilde{\boldsymbol{D}} \tag{6}$$

Algorithm 5 Anchoring

$\boldsymbol{X}^a = [\boldsymbol{x}_1 \cdots \boldsymbol{x}_a]$, $\boldsymbol{X} = [\boldsymbol{x}_1 \cdots \boldsymbol{x}_a \cdots \boldsymbol{x}_n]$
function ANCHORLOC($\tilde{\boldsymbol{X}}, \boldsymbol{X}^a$)
  Find $\boldsymbol{R} \in SO(2)$ such that $\boldsymbol{R}\tilde{\boldsymbol{x}}_2 = \boldsymbol{x}_2^a$
  Find $\boldsymbol{Q} \in SE(2)$ such that $\boldsymbol{Q}\boldsymbol{R}\tilde{\boldsymbol{x}}_3 = \boldsymbol{x}_3^a$
  $\boldsymbol{X} \leftarrow \boldsymbol{Q}\boldsymbol{R}\tilde{\boldsymbol{X}}$
  return $\boldsymbol{X}$
end function

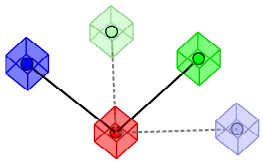

Fig. 6: In order to align the estimated positions (dashed lines) in the coordinate frame (solid), apply a rotation and a flip.

The map from the positions to distances is surjective: multiple position sets (related by an orthogonal transformation) correspond to the same EDM. Consequently, Algorithm 4 gives a set of relative positions, $\tilde{\boldsymbol{X}}$, but in an unknown frame. While robot i knows the shape of the formation, it does not know the compass direction to any particular robot j. We will consider two methods of aligning $\tilde{\boldsymbol{X}}$ in the coordinate frame: localization with anchors and localization with connected sensors.

A. Anchors

Several previous works have demonstrated the effectiveness of localization of range-only sensors using "anchor nodes" (fixed transponders with known position) [13][17][19]. We will show that this method is also useful for our approach, even if the robots do not know the exact locations of the anchor nodes. For $\mathbb{R}^2$, we require at least three non-collinear anchor nodes $\boldsymbol{x}_1^a$, $\boldsymbol{x}_2^a$, and $\boldsymbol{x}_3^a$, where the only knowledge of their configuration is the direction between $\boldsymbol{x}_1^a$ and $\boldsymbol{x}_2^a$ and the chirality of the anchor configuration: whether the path $\boldsymbol{x}_2^a \rightarrow \boldsymbol{x}_1^a \rightarrow \boldsymbol{x}_3^a$ takes a right-hand or left-hand turn. As illustrated in Figure 6, Algorithm 5 takes $\tilde{\boldsymbol{X}}$ from Algorithm 4 and first applies a rotation $\boldsymbol{R}$ by the angle between the estimated direction from anchor 1 to anchor 2 and the known direction from anchor 1 to 2 (which we define as $\hat{x}$). Then, if the new estimated position of anchor 3 is reflected about $\hat{x}$ from its known position, the algorithm applies a reflection across $\hat{x}$. Additionally, for points embedded in $\mathbb{R}^3$, a set of four non-collinear anchor nodes is necessary in order to enable a unique realization of the position set.

B. Connected Sensors

A second method to determine the coordinate frame involves mounting additional sensors in a non-collinear arrangement on each robot, for which a variant of Algorithm 5

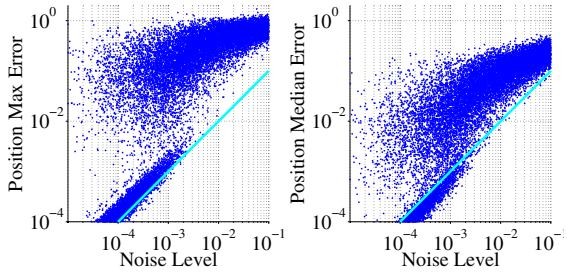

Fig. 7: Maximum and median error in estimated positions using Algorithm 2 for $n = 10$ in a 1m $\times$ 1m space, as a function of the noise level, from a Monte Carlo simulation of 20 000 trials. The cyan line denotes error that is proportional to the noise level.

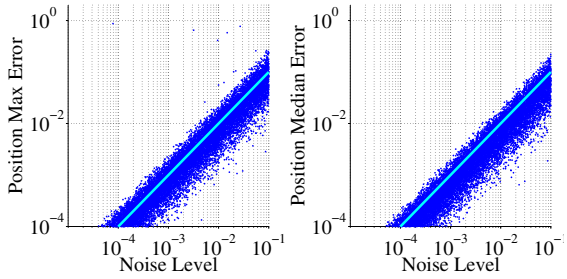

Fig. 8: Maximum and median error in estimated positions using Algorithm 3 in a 1m $\times$ 1m space (for three robots operating asynchronously), as a function of the noise level, from a Monte Carlo simulation of 20 000 trials. The cyan line denotes error that is proportional to the noise level.

also applies. If each robot contains not only a transmitter-receiver pair but also an array of additional passive receivers, then it can localize its estimates of the other robots' positions with respect to its body-fixed frame. In general, if we know the relative positions of the nodes on a platform (as opposed to knowing chirality only), we can find $\boldsymbol{R}$ that minimizes $\|\boldsymbol{R}\tilde{\boldsymbol{X}}^a - \boldsymbol{X}^a\|$, where $\boldsymbol{X}^a$ and $\tilde{\boldsymbol{X}}^a$ are the known and estimated positions of the nodes on the platform, respectively[3].

V. Simulation Results

Figures 7 and 8 show the performance of Algorithms 2 and 3, respectively, as a function of the level of noise in the system. An ideal algorithm estimates positions such that the error is at most proportional to the level of noise in the system (as in Figure 8). Under Algorithm 2, while individual nodes can have higher errors (Figure 7, left plot) due to incorrectly sorted echoes, the median error (Figure 7, right plot) remains within an acceptable range. Figures 7 and 8 demonstrate a major challenge in scaling the Acoustic Echoing Protocol. As the system size n increases, it is more likely for the AEP to make incorrect assignments. Therefore, a discrete breakdown in the accuracy of the algorithm occurs at a certain noise level, as shown in Figure 7.

The simulation results in Figures 9 and 11 use levels of noise in the regime in which there is a high probability

[3]This is known as the orthogonal Procrustes problem, first solved in [27]. Let $\boldsymbol{X}\tilde{\boldsymbol{X}}^T = \boldsymbol{U}\boldsymbol{\Lambda}\boldsymbol{V}^T$. Then, $\boldsymbol{R} = \boldsymbol{U}\boldsymbol{V}^T$.

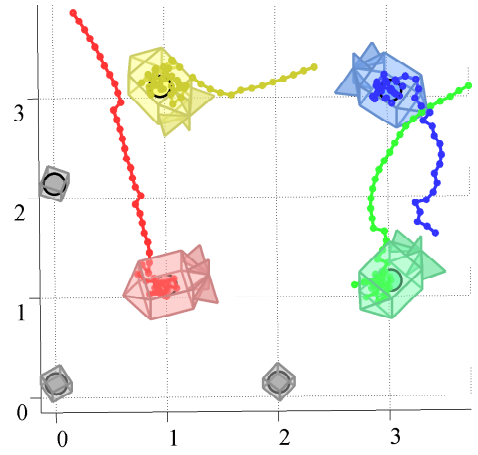

Fig. 9: Simulated trajectories for a system of four mobile robots (colored) and three anchor robots (gray) converging to a formation, with each robot independently using Algorithms 1, 2, 4, and 5 at each time step. Measurement errors are simulated as additive Gaussian noise on each recorded echo ($\mathcal{N}(0, 0.01\text{m})$).

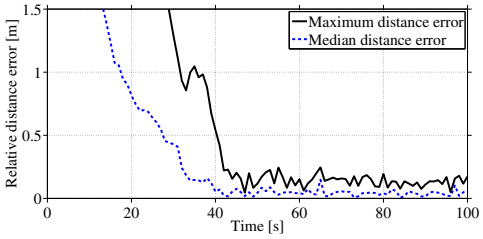

Fig. 10: Maximum and median errors between actual and desired pairwise relative distances among the robots performing formation control in Figure 9. Distance errors decay to the magnitude of the measurement noise, indicating that the system achieves the desired formation.

of mis-assigning some distances. Figure 9 demonstrates localization with anchors with the formation control scheme,

$$\dot{\boldsymbol{x}}_i = \sum_{j=1}^{n} (\boldsymbol{x}_j - \boldsymbol{x}_i) \left(\|\boldsymbol{x}_j - \boldsymbol{x}_i\| - \bar{d}_{ij} \right), \tag{7}$$

for a set of desired relative distances $\bar{d}_{ij}$. All four robots and three anchors perform the Acoustic Echoing Protocol to estimate the relative positions, and each robot is controlled based on its own measurements only. Because each localization step takes into account only the current measurements, this method places no constraints on the translation of the anchor set in space. For instance, we could consider the example of anchor nodes fixed on a surface vessel, enabling AUVs to maintain a formation with respect to the moving vessel.

Figure 11 shows simulation results for four robots (each containing one transmitter-receiver pair and two passive receivers) using the sensor-array localization method to perform the control law in (7). Each robot receives time-of-arrival measurements at three sensors and localizes the position estimates in its body-fixed coordinate frame. The noise is modeled as additive Gaussian noise ($\mathcal{N}(0, 0.1\text{m})$)

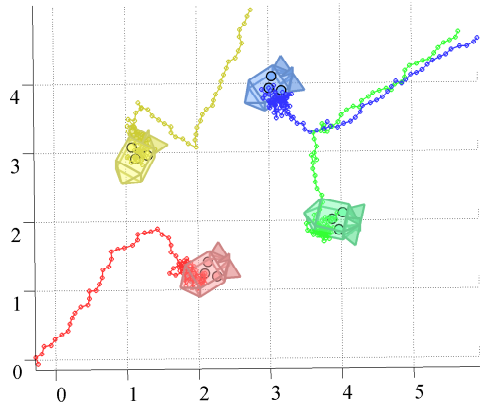

Fig. 11: Simulated trajectories for a system of four robots, each with an array consisting of one sensor-transmitter and two passive sensors. At each time step, each robot fixes its position estimates with respect to the coordinate frame of its sensor array. It then performs control according to (7), with a desired formation of a square of side length 2m. Measurement errors are simulated as additive Gaussian noise on each recorded echo ($\mathcal{N}(0, 0.1\text{m})$), and the simulation also includes Gaussian process noise at each time step ($\mathcal{N}(0, 0.1\text{m})$).

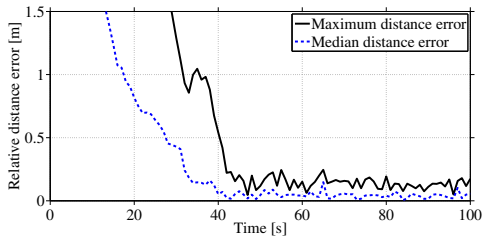

Fig. 12: Maximum and median errors between actual and desired pairwise relative distances among the robots performing formation control in Figure 11. Distance errors decay to the magnitude of the measurement noise, indicating that the system achieves the desired formation.

in the regime of unreliable echo sorting. Figure 12 shows that the robot-to-robot distances in this simulation converge to the desired values, indicating that the system reaches the prescribed formation.

VI. Conclusion

This paper has presented a method for determining the relative positions of a multi-robot system using only acoustic pulses. At each time step, each robot takes measurements and computes an estimate of the positions of the other robots in the system using only those measurements. The strategy is fully distributed and does not require robot-to-robot communication channels outside of sending and receiving acoustic pulses, making it appropriate for environments in which global positioning or high-bandwidth communication channels are unavailable (such as underwater) and for systems with limited sensing capabilities.

The primary goal of this line of research is to use range-only, communication-restricted sensing to implement distributed control of a multi-robot system. While this paper has presented two methods for resolving flip and rotational ambiguities in relative positions, each method still places additional constraints on system design. We are currently investigating a filtering-based approach to orienting relative position measurements in a robot's body frame based on changes in measurements as the robot moves.

References

[1] C. Nieto-Granda, J. G. Rogers III, and H. I. Christensen, "Coordination strategies for multi-robot exploration and mapping," *The International Journal of Robotics Research*, vol. 33, no. 4, pp. 519–533, 2014.

[2] K. Hausman, J. Müller, A. Hariharan, N. Ayanian, and G. S. Sukhatme, "Cooperative multi-robot control for target tracking with onboard sensing," *The International Journal of Robotics Research*, vol. 34, no. 13, pp. 1660–1677, 2015.

[3] J. Alonso-Mora, R. Knepper, R. Siegwart, and D. Rus, "Local motion planning for collaborative multi-robot manipulation of deformable objects," in *Robotics and Automation (ICRA), 2015 IEEE International Conference on*. IEEE, 2015, pp. 5495–5502.

[4] S. B. Williams, O. Pizarro, D. M. Steinberg, A. Friedman, and M. Bryson, "Reflections on a decade of autonomous underwater vehicles operations for marine survey at the Australian Centre for Field Robotics," *Annual Reviews in Control*, vol. 42, pp. 158–165, 2016.

[5] A. Alcocer, P. Oliveira, and A. Pascoal, "Underwater acoustic positioning systems based on buoys with GPS," in *Proceedings of the Eighth European Conference on Underwater Acoustics*, vol. 8, 2006, pp. 1–8.

[6] S. I. Roumeliotis and G. A. Bekey, "Distributed multirobot localization," *IEEE Transactions on Robotics and Automation*, vol. 18, no. 5, pp. 781–795, 2002.

[7] P. Newman and J. Leonard, "Pure range-only sub-sea SLAM," in *Robotics and Automation, 2003. Proceedings. ICRA'03. IEEE International Conference on*, vol. 2. IEEE, 2003, pp. 1921–1926.

[8] J. Djugash, S. Singh, G. Kantor, and W. Zhang, "Range-only SLAM for robots operating cooperatively with sensor networks," in *Robotics and Automation, 2006. ICRA 2006. Proceedings 2006 IEEE International Conference on*. IEEE, 2006, pp. 2078–2084.

[9] X. S. Zhou and S. I. Roumeliotis, "Robot-to-robot relative pose estimation from range measurements," *IEEE Transactions on Robotics*, vol. 24, no. 6, pp. 1379–1393, 2008.

[10] D. Moore, J. Leonard, D. Rus, and S. Teller, "Robust distributed network localization with noisy range measurements," in *Proceedings of the 2nd international conference on Embedded networked sensor systems*. ACM, 2004, pp. 50–61.

[11] M. F. Fallon, G. Papadopoulos, J. J. Leonard, and N. M. Patrikalakis, "Cooperative AUV navigation using a single maneuvering surface craft," *The International Journal of Robotics Research*, vol. 29, no. 12, pp. 1461–1474, 2010.

[12] A. Cornejo and R. Nagpal, "Distributed range-based relative localization of robot swarms," in *Algorithmic Foundations of Robotics XI*. Springer, 2015, pp. 91–107.

[13] R. Rangarajan, R. Raich, and A. O. Hero, "Euclidean matrix completion problems in tracking and geo-localization," in *Acoustics, Speech and Signal Processing, 2008. ICASSP 2008. IEEE International Conference on*. IEEE, 2008, pp. 5324–5327.

[14] S. Srirangarajan, A. H. Tewfik, and Z.-Q. Luo, "Distributed sensor network localization with inaccurate anchor positions and noisy distance information," in *Acoustics, Speech and Signal Processing, 2007. ICASSP 2007. IEEE International Conference on*, vol. 3. IEEE, 2007, pp. 521–524.

[15] P. Oguz-Ekim, J. P. Gomes, J. Xavier, and P. Oliveira, "Robust localization of nodes and time-recursive tracking in sensor networks using noisy range measurements," *IEEE Transactions on Signal Processing*, vol. 59, no. 8, pp. 3930–3942, 2011.

[16] J. C. Gower, "Euclidean distance geometry," *Math. Sci*, vol. 7, no. 1, pp. 1–14, 1982.

[17] I. Dokmanic, R. Parhizkar, J. Ranieri, and M. Vetterli, "Euclidean distance matrices: essential theory, algorithms, and applications," *IEEE Signal Processing Magazine*, vol. 32, no. 6, pp. 12–30, 2015.

[18] I. Dokmanić, Y. M. Lu, and M. Vetterli, "Can one hear the shape of a room: The 2D polygonal case," in *Acoustics, Speech and Signal Processing (ICASSP), 2011 IEEE International Conference on*. IEEE, 2011, pp. 321–324.

[19] I. Dokmanić, R. Parhizkar, A. Walther, Y. M. Lu, and M. Vetterli, "Acoustic echoes reveal room shape," *Proceedings of the National Academy of Sciences*, vol. 110, no. 30, pp. 12 186–12 191, 2013.

[20] I. Dokmanić, L. Daudet, and M. Vetterli, "How to localize ten microphones in one finger snap," in *Signal Processing Conference (EUSIPCO), 2014 Proceedings of the 22nd European*. IEEE, 2014, pp. 2275–2279.

[21] I. Dokmanić, J. Ranieri, and M. Vetterli, "Relax and unfold: Microphone localization with Euclidean distance matrices," in *Signal Processing Conference (EUSIPCO), 2015 23rd European*. IEEE, 2015, pp. 265–269.

[22] O. Oçal, I. Dokmanic, and M. Vetterli, "Source localization and tracking in non-convex rooms," in *Acoustics, Speech and Signal Processing (ICASSP), 2014 IEEE International Conference on*. IEEE, 2014, pp. 1429–1433.

[23] I. Dokmanić, L. Daudet, and M. Vetterli, "From acoustic room reconstruction to SLAM," in *Acoustics, Speech and Signal Processing (ICASSP), 2016 IEEE International Conference on*. IEEE, 2016, pp. 6345–6349.

[24] M. Kreković, I. Dokmanić, and M. Vetterli, "EchoSLAM: Simultaneous localization and mapping with acoustic echoes," in *Acoustics, Speech and Signal Processing (ICASSP), 2016 IEEE International Conference on*. IEEE, 2016, pp. 11–15.

[25] ——, "Omnidirectional bats, point-to-place distances, and the price of uniqueness," in *42nd International Conference on Acoustics, Speech and Signal Processing*, no. EPFL-CONF-221397, 2017.

[26] J. Borish, "Extension of the image model to arbitrary polyhedra," *The Journal of the Acoustical Society of America*, vol. 75, no. 6, pp. 1827–1836, 1984.

[27] P. H. Schönemann, "A generalized solution of the orthogonal Procrustes problem," *Psychometrika*, vol. 31, no. 1, pp. 1–10, 1966.